2015

The influence of charge and magnetic order on polaron and acoustic phonon dynamics in $LuFe_2O_4$

J. Lee
Los Alamos National Laboratory, kjindda@naver.com

S. A. Trugman
Los Alamos National Laboratory

C. L. Zhang
Rutgers University

D. Talbayev
Tulane University of Louisiana

Xiaoshan Xu
University of Nebraska-Lincoln, xiaoshan.xu@unl.edu

See next page for additional authors

The influence of charge and magnetic order on polaron and acoustic phonon dynamics in $LuFe_2O_4$

J. Lee,[1,a)] S. A. Trugman,[1,2] C. L. Zhang,[3] D. Talbayev,[4] X. S. Xu,[5] S.-W. Cheong,[3] D. A. Yarotski,[1] A. J. Taylor,[1] and R. P. Prasankumar[1,b)]
[1]*Center for Integrated Nanotechnologies, Los Alamos National Laboratory, Los Alamos, New Mexico 87545, USA*
[2]*Theoretical Division, Los Alamos National Laboratory, Los Alamos, New Mexico 87545, USA*
[3]*Rutgers Center for Emergent Materials and Department of Physics and Astronomy, Rutgers University, Piscataway, New Jersey 08854, USA*
[4]*Department of Physics and Engineering Physics, Tulane University, New Orleans, Louisiana 70118, USA*
[5]*Department of Physics and Astronomy, Nebraska Center for Materials and Nanoscience, University of Nebraska, Lincoln, Nebraska 68588, USA*

(Received 23 March 2015; accepted 14 July 2015; published online 29 July 2015)

Femtosecond optical pump-probe spectroscopy is used to reveal the influence of charge and magnetic order on polaron dynamics and coherent acoustic phonon oscillations in single crystals of charge-ordered, ferrimagnetic $LuFe_2O_4$. We experimentally observed the influence of magnetic order on polaron dynamics. We also observed a correlation between charge order and the amplitude of the acoustic phonon oscillations, due to photoinduced changes in the lattice constant that originate from the photoexcited electrons. This provides insight into the general behavior of coherent acoustic phonon oscillations in charge-ordered materials. © *2015 AIP Publishing LLC*. [http://dx.doi.org/10.1063/1.4927739]

Multiferroic materials have attracted much recent attention due to the strong coupling between their electric and magnetic degrees of freedom, which is interesting from a fundamental perspective as well as for potential applications in magnetoelectric and magneto-optical devices. Multiferroics simultaneously possesses spontaneous electric and magnetic order, which can be switched by the corresponding applied electric and magnetic fields, respectively. However, the simultaneous presence of electric and magnetic polarization alone does not necessitate strong coupling between these two properties, since they derive from two different broken symmetries (magnetism from breaking time reversal symmetry and ferroelectricity (FE) from breaking spatial inversion symmetry[1]). Microscopically, magnetism in multiferroics originates from partially filled *d* or *f* shells in localized atoms, but ferroelectricity can originate from several different mechanisms (such as lattice distortions, lone pairs, spin spirals, and charge ordering (CO)).[2]

The prototypical charge-ordered multiferroic $LuFe_2O_4$ has recently attracted much attention due to its extensive dielectric tunability and potential for magnetoelectric (ME) coupling near room temperature,[3,4] making it promising for various applications in magnetically controlled ferroelectric devices[3] and electrically controlled magnetic memory and sensing devices.[2] For example, $LuFe_2O_4$ has already been used as a novel multiferroic substrate for tuning the surface-enhanced Raman scattering response in Au nanostructures.[5] The unit cell of $LuFe_2O_4$ consists of three Fe_2O_4 bilayers (known as W layers[6]) with single Lu_2O_3 layers sandwiched between different bilayers, as shown in Figure 1(a). Initial studies revealed bulk ferroelectric order below the charge ordering temperature, $T_{CO} \sim 320$ K, resulting in a spontaneous electric polarization that further increased upon the appearance of ferrimagnetic spin order below the Neel temperature, $T_N \sim 240$ K.[3] Ferroelectricity in each bilayer is thus believed due to CO, although the orientation of the FE polarization between adjacent bilayers (Figure 1(b)) (and thus the existence of a macroscopic FE polarization[3]) is still controversial,[7] as experimental evidence for an antiferroelectric ground state has also been observed.[8,9] Theoretical

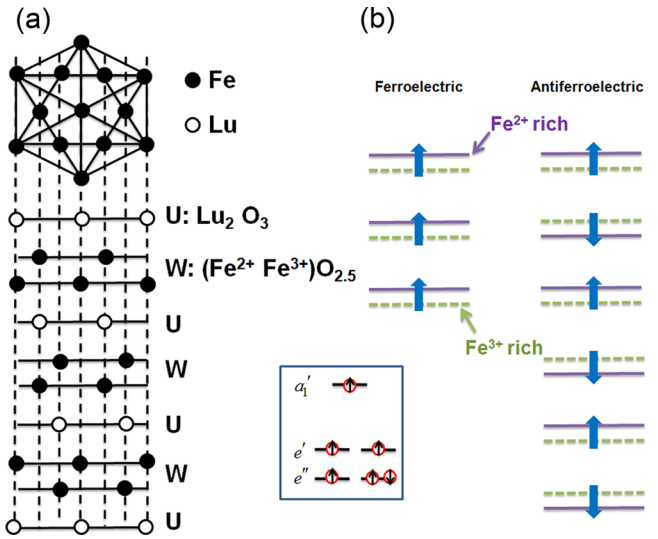

FIG. 1. (a) A side view of the $LuFe_2O_4$ crystal structure, with oxygen ions omitted for simplicity. Adapted with permission from Iida *et al.*, J. Phys. Soc. Jpn. **62**, 1723 (1993). Copyright 1993 Journal of the Physical Society of Japan. U denotes single Lu_2O_3 layers and W denotes Fe_2O_4 bilayers. The top part of (a) shows a top view of the crystal structure. (b) Schematic of two different ground states, ferroelectric and antiferroelectric, for $T < T_{CO}$ in the $LuFe_2O_4$ unit cell. The inset shows a schematic of the energy levels for Fe^{2+}, including the crystal field splitting.

a)Email: kjindda@naver.com
b)Email: rpprasan@lanl.gov

explanations for the proposed antiferroelectric and ferroelectric orders were given in Refs. 9 and 10, respectively.

Here, we present femtosecond optical pump-probe measurements of polaron and acoustic phonon dynamics in $LuFe_2O_4$, obtained by measuring the transient photoinduced change in reflectivity ($\Delta R/R$) at 1.1 eV (which probes the Fe^{2+} to Fe^{3+} interlayer site-to-site polaronic excitation[11–13]) after degenerately pumping the same transition energy. We observe a fast relaxation component attributed to polaron dynamics that is influenced by the development of spin order, as well as a slower oscillating component that substantially changes across the CO transition. We show that these oscillations are due to the generation of coherent acoustic phonons through the electronic deformation potential, driven by photoinduced changes in the electron temperature. Our study thus further demonstrates that ultrafast optical pump-probe spectroscopy can reveal changes in material properties across a charge-ordering transition through their influence on acoustic phonon oscillations, which underlines the importance of this technique for providing insight into the exotic properties of strongly correlated materials.[14,15] Finally, our results shed light on the interplay between the lattice, magnetic, and electronic degrees of freedom in $LuFe_2O_4$ and the ultimate speed limitations when using it in various applications.

Our femtosecond optical pump-probe spectroscopy system is based on a 75 fs, 250 kHz repetition rate amplified Ti:sapphire laser system operating at 800 nm (1.55 eV), and seeding an optical parametric amplifier (OPA) that allows us to tune the photon energy to 1.1 eV.[12] Temperature-dependent transient reflectivity changes were obtained in reflection with cross-polarized pump and probe beams at a >10:1 power ratio. The pump beam was incident parallel to the surface normal (which is parallel to the c-axis of the crystal) and the probe beam was incident at an angle of $<10^\circ$ to normal. A delay line enables us to vary the optical path difference between the pump and probe beams, which are then focused to the same spot on the sample with beam diameters of 200 and 100 μm, respectively. The amplitude of the $\Delta R/R$ signal changes linearly with pump fluence over the range examined here ($\sim$13–115 $\mu J/cm^2$). The pump fluence for the data discussed in the remainder of the paper was 76 $\mu J/cm^2$ (photoexciting $\sim$0.007 electrons/unit cell), which transiently increased the sample temperature by $\sim$10 K throughout the measured temperature range (calculated using the heat capacity in Ref. 16). This should not significantly affect the measured dynamics, as the sample completely recovers in the 4 μs time interval between amplifier pulses. The $LuFe_2O_4$ single crystal used in this study was grown by the floating zone method, described in more detail in Ref. 17.

Figure 2(a) shows the temporal profile of the normalized photoinduced reflectivity change, $\Delta R/R(t)$, in $LuFe_2O_4$ at several different temperatures for a degenerate 1.1 eV pump-probe measurement. Following photoexcitation, $\Delta R/R$ decreases to its minimum value within $\lesssim$0.5 ps (Fig. 2(b)) after which it recovers on both fast and slow timescales, clearly exhibiting strong oscillations while returning to equilibrium. The $\Delta R/R$ trace can be fitted with a standard equation incorporating two exponentially decaying terms,[18] which allows us to obtain the fast (τ_{fast}) and slow (τ_{slow}) decay time constants and also separately extract the oscillatory component, as discussed in more detail below.

In many strongly correlated electron systems, the fast component of the photoinduced reflectivity change is believed due to the photoexcitation and rapid re-trapping of electrons into polaronic states.[19,20] This is also expected to be the case for $LuFe_2O_4$, since previous work has shown that 1.1 eV photons excite small polarons that hop between layers from Fe^{2+} to Fe^{3+} sites.[11] More specifically, the crystal field from the FeO_5 bipyramidal structure causes the Fe 3d levels in $LuFe_2O_4$ to split into two doublets, e'' (d_{zx}, d_{yz}) and e' (d_{xy}, $d_{x^2-y^2}$), and a singlet, a_1' ($d_{3z^2-r^2}$), as shown in the inset of Fig. 1.[21] When the sample is photoexcited at 1.1 eV, a polaronic carrier in an e'' level on a Fe^{2+} site in one layer can hop to an e'' state on the nearest Fe^{3+} site in the adjacent layer. This change in the charge state of the Fe^{2+} and Fe^{3+} ions then initiates the motion of the surrounding negatively charged oxygen atoms (as the Coulomb interaction causes them to change their position relative to the Fe ions, depending on the amount of charge on a given Fe ion), which then re-trap the electron into a polaronic state. The relaxation time, τ_{fast} (Figures 2(b) and 2(c)), of the electron-lattice interaction in $LuFe_2O_4$ then corresponds to this recovery of a photoexcited electron to the polaronic state. Our measurements show that $\tau_{fast} \sim$ 200–400 fs in $LuFe_2O_4$, with the longest relaxation times occurring near T_N as shown in Figure 2(c), suggesting that magnetic order influences polaron

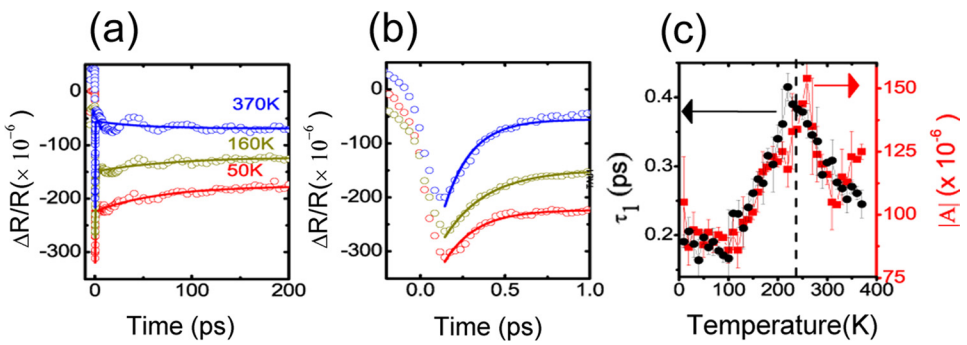

FIG. 2. (a) Transient reflectivity of the 1.1 eV probe pulse. The open circles are the experimentally obtained data points and the solid lines show the result of fitting the data with two exponential terms. Each trace is shifted along the y axis by a constant value to facilitate comparisons between them. (b) The data from (a) at early times. (c) The fast decay time constant (black) and the magnitude of the minimum amplitude of the fast decay term (red) as a function of temperature, revealing a peak at T_N. The vertical dashed line shows T_N.

dynamics in this system. The magnitude of the minimum amplitude of fast decay component also rapidly changes in the vicinity of T_N, consistent with the rapid onset of spin ordering in this material (Figure 2(c), blue curve).

One possible explanation for the observed fast dynamics is the intrinsic spatial inhomogeneity that develops near T_N through the formation of oppositely oriented clusters of spins.[22] At low temperatures ($T < T_N$), charge and spin order would prevent an electron photoexcited from a Fe^{3+} site in the bottom layer to a Fe^{2+} site in the top layer from hopping to any other nearest neighbour sites (see, e.g., Fig. 3 in Ref. 12). However, as T increases towards T_N, a photoexcited electron could cross into an oppositely oriented spin cluster and hop to additional sites, effectively increasing its lifetime. Furthermore, the size of these clusters, given by the magnetic correlation length, should peak at T_N,[23] qualitatively agreeing with the temperature dependence of the fast time constant in Fig. 2(c). The influence of AFM order on polaron trapping could also affect the observed sub-picosecond relaxation.[24] Finally, we note that charge order could also influence polaron dynamics, which may be the origin of the small plateau in the fast decay time constant above 320 K; however, we did not take enough data points in this range to draw any definitive conclusions. The investigation of these and other possibilities for explaining the sub-picosecond dynamics will be the subject of future work; for the remainder of this paper, we will focus on analyzing the observed oscillations in the $\Delta R/R$ signal to gain more insight into the physics of $LuFe_2O_4$.

Figure 3(a) shows the oscillations (fitted with an equation of the form $De^{-t/\tau_d}\sin\left(\frac{2\pi t}{\tau_p}+\phi\right)$) extracted from our data by subtracting the fast (τ_{fast}) and slow (τ_{slow}) decay terms, where τ_p is the oscillation period. We note that τ_{slow} (on the order of 200 ps in $LuFe_2O_4$) is typically attributed to heating in most ultrafast experiments on correlated electron materials, although electron-hole recombination can also play a role;[25] we will not discuss this decay process further here. The observed oscillations are typically attributed to coherent acoustic phonons, which can be manifested as propagating strain waves, generated through the dynamic stress induced by absorption of the femtosecond laser pulses within

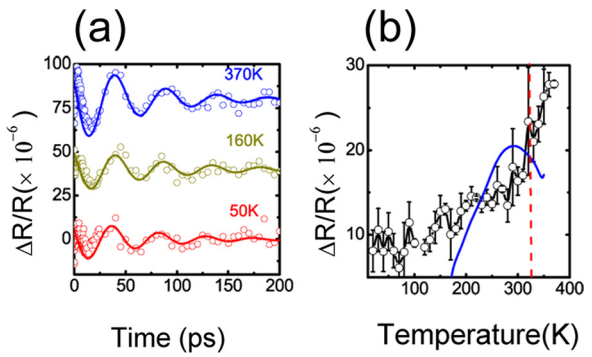

FIG. 3. (a) The residual coherent oscillations after subtracting the double exponential decay terms from Figure 2(a). (b) Oscillation amplitude as a function of temperature; the red dashed line denotes the charge ordering temperature T_{CO} and the blue solid line is the calculated phonon-induced change in the lattice constant, $|dl_C(T)/dT|\Delta Q/C(T)$, using a constant scaling factor for comparison. The temperature dependent $dl_C(T)/dT$ and $C(T)$ terms were obtained from Refs. 33 and 16, respectively.

the penetration depth.[26] These strain waves have often been observed in ultrafast optical experiments on correlated electron materials[27–29] and semiconductors,[30,31] with an oscillation period that depends on the probe wavelength, given by

$$\tau_p = \lambda/(2nV_s), \tag{1}$$

where λ, n, and V_s are the probe wavelength, refractive index ($n \approx 2$ (Ref. 11)), and c-axis sound velocity, respectively,[27–31] and the measured oscillation period $\tau_p \sim 48$ ps. In our experiments, doubling the probe photon energy caused the oscillation frequency to double, supporting coherent acoustic phonon generation as the origin of the oscillations.[26] The measured oscillation frequency of 20.8 GHz only minimally depends on temperature, as does the refractive index,[11] allowing us to find that $V_s = 5.88 \times 10^5$ cm/s over a broad temperature range, comparable to that measured in manganites.[32]

Figure 3(a) reveals that the oscillations are damped with a time constant of $\tau_d \sim 70$ ps (obtained from the curve fit) that only weakly depends on temperature. This is primarily due to the finite penetration depth of the probe light ($l_p \sim 0.82\ \mu$m at 1.1 eV).[26,27,31] Essentially, the strain wave is generated near the surface, after which it propagates into the material at a speed of V_s, causing the signals shown in Figure 3(a) to decay over a distance of $l_d \sim 0.4\ \mu$m (calculated from τ_d and V_s). This is comparable to half of the light penetration depth (0.41 μm), allowing us to conclude that the damping of the oscillation originates from absorption of our 1.1 eV probe pulses.

The temperature dependence of the oscillation amplitude is plotted in Figure 3(b), showing that the slope gets steeper near and above T_{CO}. This is somewhat unexpected given that the penetration depth in $LuFe_2O_4$ at 1.1 eV does not change significantly with temperature,[11] and we used the same pump fluence over the full measured temperature range. More insight can be obtained by considering the possibility that the strain wave is generated by photoinduced changes in the c-axis lattice constant, l_C.[29] This can be described by the equation

$$\Delta l_C(t) = \frac{\partial l_C(t)}{\partial T_p(t)}\Delta T_p(t) + \frac{\partial l_C(t)}{\partial T_e(t)}\Delta T_e(t), \tag{2}$$

where Δl_C, ΔT_e and ΔT_p are the photoinduced change in the lattice constant and the electron and phonon temperatures, respectively.[26] We start by considering the first term, which describes a photoinduced modification of the lattice constant through a transient increase in the phonon temperature. This occurs through the relaxation of photoexcited carriers to the band minima through incoherent scattering with phonons and can be approximated by $\Delta l_C \sim |dl_C(T)/dT|\Delta Q/C(T)$, where ΔQ and $C(T)$ are the energy from the pump beam and the specific heat of $LuFe_2O_4$, respectively.[29] This expression can then be used to estimate the change in l_C from increasing the phonon temperature. As shown in Ref. 33, l_C does not change significantly with temperature (from 25.26 Å at low temperatures ($T \ll T_{CO}$) to 25.23 Å at high temperatures ($T > T_{CO}$)), giving $dl_C(T)/dT \sim 2.2 \times 10^{-4}$ Å/T. Furthermore, as mentioned above, the photoinduced temperature increase for the pump fluence used here is ~10 K, resulting in a rather small phonon-induced change in the lattice constant (e.g.,

$\Delta l_C \sim 2.2 \times 10^{-3}$ Å at ~240 K (where $C(T) \sim 160$ J/K/mol (Ref. 16))). The blue solid line in Figure 3(b) shows the change in lattice constant in $LuFe_2O_4$ calculated using this expression, revealing a large discrepancy between our data and the fitted values. Most notably, for $T > T_{CO}$ the measured oscillation amplitude continues to increase, but the calculated values peak near T_{CO} and decrease at higher temperatures (as in Ref. 29). It is therefore difficult to explain the increase in oscillation amplitude near T_{CO} through changes in l_C that are induced solely by transient increases in the phonon temperature.

One can instead consider changes in l_C due to heating *electrons*; i.e., energy transfer to the electronic subsystem, which has a relatively small heat capacity,[34] from femtosecond photoexcitation could result in a large temperature change within the first few hundred femtoseconds. In fact, our 1.1 eV photoexcitation would result in an initial carrier (electrons plus holes) temperature of a few thousand Kelvin. This would then directly modify the lattice constant of each unit cell via the deformation potential[26] (Eq. (2)), launching an initially coherent lattice constant change as all ~324 unit cells (along the *c*-axis) photoexcited by the pump pulse (calculated from $l_p \sim 0.82\,\mu$m) expand or contract in phase with one another; we note that the magnitude of the photoinduced lattice expansion per unit cell will decrease with increasing depth, due to absorption of the pump pulse. This excitation is clearly delocalized in space and therefore will initially generate coherent phonons with momentum close to $k \sim 0$. If the time resolution is high enough, then both $k \sim 0$ coherent optical[14] and acoustic phonons[27–29] can be detected. However, we were unable to detect any coherent optical phonons, due to our relatively low time resolution (~75 fs) and their frequencies of several terahertz. The actual oscillation shown in the data is thus likely to be due to $k \sim 0$ coherent acoustic phonons generated by the hot electron population.

The amplitude of these coherent acoustic phonon oscillations (Figure 3(a)) will thus depend on the magnitude of the change in lattice constant induced by photoexcited electrons. This can be understood by using a simple diatomic one-dimensional lattice structure, supporting one coherent longitudinal acoustic phonon mode, to model the arrangement of $LuFe_2O_4$ bilayers along the *c* axis (whether they are arranged in a ferroelectric or antiferroelectric manner) (Figure 3(c)).[35] As described above, the 1.1 eV pump photons will be absorbed by the shorter bonds, since 1.1 eV corresponds to an excitation from the bottom to the top layer. Above T_{CO}, when there is no charge order, this corresponds to a transition between bonding and anti-bonding orbitals, which will increase the lattice spacing. To elucidate this point in more detail, we consider a simple two-ion system with only one electronic energy level on each site, as described by Eq. (3) in Ref. 13,

$$H^1 = \begin{pmatrix} \varepsilon_1 & -t \\ -t & \varepsilon_2 \end{pmatrix}, \tag{3}$$

where ε_i is the atomic energy at site i ($i = 1,2$) and t is a matrix element accounting for the hopping between the two sites. Above T_{CO}, in a symmetric two site tight-binding model, the molecular orbitals will have bonding and anti-bonding states.[36] Since the two atomic sites are identical, $\varepsilon_1 = \varepsilon_2$, and the energy for transitions between the bonding and anti-bonding states is proportional to t. One can then approximate the dependence of the hopping matrix element t on the bond length r using $t \sim \exp(-r)$.[37] This expression shows that the energy decreases rapidly with increasing r, providing a strong incentive for the system to increase the bond length above T_{CO}.

In contrast, below T_{CO} the excitation is due to interlayer charge transfer from Fe^{2+} to Fe^{3+} ions, which will not induce as large a lattice expansion as at higher T ($T > T_{CO}$). This can be seen by considering that the sites are not identical below T_{CO}; therefore, since $|\varepsilon_2 - \varepsilon_1| \gg t$, the excited state eigenvalue is approximately ε_2 (when $\varepsilon_2 > \varepsilon_1$), which is approximately independent of t and thus of r. There is thus little energetic benefit to reduce the bond length in this temperature range. Overall, these considerations could explain the observed stronger oscillations at high temperature. Finally, we note that the relatively gradual variation in the oscillation amplitude across T_{CO} is consistent with the trends observed in other measurements (e.g., the specific heat[16] and lattice constant[33]). This may be due to the fact that short-range charge order can be maintained in each bilayer well above T_{CO}.[9]

More generally, similar trends have been observed using femtosecond spectroscopy to study other charge-ordered materials, such as $La_{0.5}Ca_{0.5}MnO_3$ and $La_{1/4}Pr_{3/8}Ca_{3/8}MnO_3$, although changes in the phonon temperature were only considered on longer time scales.[28,29] These systems also show a strong decrease in the amplitude of acoustic phonon oscillations as the temperature is reduced below T_{CO}, with a corresponding increase in the amplitude of optical phonon oscillations. This could also be explained in a similar manner to $LuFe_2O_4$, as the lattice constant can also change through electronic transitions for $T > T_{CO}$ in those manganites, thus decreasing the measured acoustic phonon oscillation amplitude as the temperature is varied below T_{CO}.

In conclusion, we used ultrafast optical spectroscopy to examine polaron and acoustic phonon dynamics in $LuFe_2O_4$. We observe a sub-picosecond relaxation that corresponds to the photoexcitation and redressing of lattice polarons, along with coherent acoustic phonon oscillations that show a strong amplitude change across T_{CO}. This can be associated with a simultaneous change in the lattice constant induced by changes in the electron temperature, which strongly influences the amplitude of the coherent acoustic phonon oscillations. Our study thus provides further evidence that ultrafast optical pump-probe spectroscopy is an important technique for investigating the unique properties of strongly correlated materials and can provide insight relevant to future applications.

We would like to thank Cristian Batista for helpful discussions. This work was performed at the Center for Integrated Nanotechnologies, a U.S. Department of Energy, Office of Basic Energy Sciences (BES) user facility and supported by the Laboratory Directed Research and Development program at LANL. Los Alamos National Laboratory, an affirmative action equal opportunity employer, is operated by Los Alamos National Security, LLC, for the National Nuclear Security administration of the U.S. Department of Energy under Contract No. DE-AC52-06NA25396. The work at Rutgers University was supported by the DOE under Grant No. DE-FG02-07ER46382.

[1]J. van den Brink and D. Khomskii, J. Phys.: Condens. Matter **20**, 434217 (2008).
[2]D. Khomskii, Physics **2**, 20 (2009).
[3]N. Ikeda, H. Ohsumi, K. Ohwada, K. Ishii, T. Inami, K. Kakurai, Y. Murakami, K. Yoshii, S. Mori, Y. Horibe, and H. Kitô, Nature **436**, 1136 (2005).
[4]M. A. Subramanian, T. He, J. Chen, N. S. Rogado, T. G. Calvarese, and A. W. Sleight, Adv. Mater. **18**, 1737 (2006).
[5]X. Xu, K. Seal, X. Xu, I. Ivanov, C. H. Hsueh, N. A. Hatab, L. Yin, X. Zhang, Z. Cheng, B. Gu, Z. Zhang, and J. Shen, Nano Lett. **11**, 1265 (2011).
[6]J. Iida, M. Tanaka, Y. Nakagawa, S. Funahashi, N. Kimizuka, and S. Takekawa, J. Phys. Soc. Jpn. **62**, 1723 (1993).
[7]S. M. Gaw, H. J. Lewtas, D. F. McMorrow, J. Kulda, R. A. Ewings, T. G. Perring, R. A. McKinnon, G. Balakrishnan, D. Prabhakaran, and A. T. Boothroyd, Phys. Rev. B **91**, 035103 (2015).
[8]X. S. Xu, J. de Groot, Q.-C. Sun, B. C. Sales, D. Mandrus, M. Angst, A. P. Litvinchuk, and J. L. Musfeldt, Phys. Rev. B **82**, 014304 (2010).
[9]M. Angst, R. P. Hermann, A. D. Christianson, M. D. Lumsden, C. Lee, M.-H. Whangbo, J.-W. Kim, P. J. Ryan, S. E. Nagler, W. Tian, R. Jin, B. C. Sales, and D. Mandrus, Phys. Rev. Lett. **101**, 227601 (2008).
[10]H. J. Xiang and M.-H. Whangbo, Phys. Rev. Lett. **98**, 246403 (2007).
[11]X. S. Xu, M. Angst, T. V. Brinzari, R. P. Hermann, J. L. Musfeldt, A. D. Christianson, D. Mandrus, B. C. Sales, S. McGill, J.-W. Kim, and Z. Islam, Phys. Rev. Lett. **101**, 227602 (2008).
[12]J. Lee, S. A. Trugman, C. D. Batista, C. L. Zhang, D. Talbayev, X. S. Xu, S.-W. Cheong, D. A. Yarotski, A. J. Taylor, and R. P. Prasankumar, Sci. Rep. **3**, 2654 (2013).
[13]J. Lee and R. P. Prasankumar, Eur. Phys. J. B **87**, 267 (2014).
[14]S. Wall, D. Prabhakaran, A. T. Boothroyd, and A. Cavalleri, Phys. Rev. Lett. **103**, 97402 (2009).
[15]J. Zhang and R. D. Averitt, Annu. Rev. Mater. Res. **44**, 19 (2014).
[16]F. Wang, J. Kim, and Y.-J. Kim, Phys. Rev. B **80**, 024419 (2009).
[17]W. Wu, V. Kiryukhin, H.-J. Noh, K.-T. Ko, J.-H. Park, W. Ratcliff II, P. A. Sharma, N. Harrison, Y. J. Choi, Y. Horibe, S. Lee, S. Park, H. T. Yi, C. L. Zhang, and S.-W. Cheong, Phys. Rev. Lett. **101**, 137203 (2008).
[18]D. J. Hilton, "Ultrafast pump-probe spectroscopy," in *Optical Techniques for Solid-State Materials Characterization*, edited by R. P. Prasankumar and A. J. Taylor (CRC Press, 2011), Chap. 9.
[19]R. P. Prasankumar, S. Zvyagin, K. V. Kamenev, G. Balakrishnan, D. M. Paul, A. J. Taylor, and R. D. Averitt, Phys. Rev. B **76**, 020402 (2007).
[20]K. H. Wu, T. Y. Hsu, H. C. Shih, Y. J. Chen, C. W. Luo, T. M. Uen, J.-Y. Lin, J. Y. Juang, and T. Kobayashi, J. Appl. Phys. **105**, 043901 (2009).
[21]K.-T. Ko, H.-J. Noh, J.-Y. Kim, B.-G. Park, J.-H. Park, A. Tanaka, S. B. Kim, C. L. Zhang, and S-W. Cheong, Phys. Rev. Lett. **103**, 207202 (2009).
[22]R. P. Prasankumar, H. Okamura, H. Imai, Y. Shimakawa, Y. Kubo, S. A. Trugman, A. J. Taylor, and R. D. Averitt, Phys. Rev. Lett. **95**, 267404 (2005).
[23]P. M. Chaikin and T. C. Lubensky, *Principles of Condensed Matter Physics* (Cambridge University Press, Cambridge, 1995).
[24]L. Vidmar, J. Bonca, and S. Maekawa, Phys. Rev. B **79**, 125120 (2009).
[25]Y.-M. Sheu, S. A. Trugman, Y.-S. Park, S. Lee, H. T. Yi, S.-W. Cheong, Q. X. Jia, A. J. Taylor, and R. P. Prasankumar, Appl. Phys. Lett. **100**, 242904 (2012).
[26]C. Thomsen, H. T. Grahn, H. J. Maris, and J. Tauc, Phys. Rev. B **34**, 4129 (1986).
[27]D. Lim, R. D. Averitt, J. Demsar, A. J. Taylor, N. Hur, and S. W. Cheong, Appl. Phys. Lett. **83**, 4800 (2003).
[28]K.-J. Jang, J. Lim, J. Ahn, J.-H. Kim, K.-J. Yee, and J. S. Ahn, Phys. Rev. B **81**, 214416 (2010).
[29]D. Lim, V. K. Thorsmølle, R. D. Averitt, Q. X. Jia, K. H. Ahn, M. J. Graf, S. A. Trugman, and A. J. Taylor, Phys. Rev. B **71**, 134403 (2005).
[30]R. Liu, G. D. Sanders, C. J. Stanton, C. S. Kim, J. S. Yahng, Y. D. Jho, K. J. Yee, E. Oh, and D. S. Kim, Phys. Rev. B **72**, 195335 (2005).
[31]J. K. Miller, J. Qi, Y. Xu, Y.-J. Cho, X. Liu, J. K. Furdyna, I. Perakis, T. V. Shahbazyan, and N. Tolk, Phys. Rev. B **74**, 113313 (2006).
[32]R. K. Zheng, C. F. Zhu, J. Q. Xie, and X. G. Li, Phys. Rev. B **63**, 024427 (2000).
[33]Y. Hou, Y. P. Yao, S. N. Dong, M. L. Teng, X. F. Sun, and X. G. Li, J. Raman Spectrosc. **42**, 1695 (2011).
[34]O. B. Wright, Phys. Rev. B **49**, 9985 (1994).
[35]N. W. Ashcroft and N. D. Mermin, *Solid State Physics* (Harcourt, 1976).
[36]S. Blundell, *Magnetism in Condensed Matter* (Oxford, New York, 2008).
[37]F. Duan and J. Guojun, *Introduction to Condensed Matter Physics* (World Scientific, Singapore, 2005).